

Ultrafast Fluence-Reversal Fingerprint of Fragile Kondo Hybridization in CePt₂In₇

Xin-Yi Tian,¹ Qi-Yi Wu,¹ Chen Zhang,¹ Hao Liu,¹ Yang Luo,¹ Bo Chen,¹ Ying Zhou,¹ Zhong-Tuo Fu,¹ Jin-Dong Bai,¹ Chun-Hui Lyu,¹ Zi-Jie Xu,¹ Hai-Long Deng,¹ Hai-Yun Liu,² Jun He,¹ Yu-Xia Duan,¹ and Jian-Qiao Meng^{1,*}

¹*School of Physics, Central South University, Changsha 410083, Hunan, China*

²*Beijing Academy of Quantum Information Sciences, Beijing 100085, China*

(Dated: Wednesday 1st July, 2026)

The emergence of heavy quasiparticles in a Kondo lattice is usually viewed as the formation of a low-energy hybridization gap. Whether this gap represents a rigid electronic structure or a fragile many-body state that can be dynamically reconfigured remains a central question for heavy-fermion systems near magnetic order, quantum criticality, and unconventional superconductivity. Here we use femtosecond pump-probe reflectivity to interrogate this problem in the weakly hybridized Kondo-lattice compound CePt₂In₇. At low fluence, a slow quasiparticle relaxation channel emerges below $T^* \sim 40$ K and follows a Rothwarf-Taylor bottleneck response with a low-energy recombination scale $2\Delta \approx 7.4$ meV. Coherent optical phonons, independently identified by Raman spectroscopy, act as an internal lattice thermometer and rule out large quasi-equilibrium lattice heating as the origin of the nonlinear electronic response. The phonon-free electronic amplitude A_{elec} reveals a fluence-reversal fingerprint: with cooling from the hybridization-crossover regime, the response evolves from weak-linear behavior to Rothwarf-Taylor-like bottleneck suppression and finally to anomalous high-fluence enhancement at the lowest temperatures. This reversal cannot be accounted for by a rigid fixed-gap bottleneck alone and instead identifies an ultrafast optical signature of photoinduced redistribution of a fragile Kondo-hybridized electronic response.

Heavy-fermion metals pose a fundamental problem in correlated-electron physics: how do nearly localized f moments become part of an itinerant many-body electronic fluid, and how robust is that fluid once it forms? In a Kondo lattice, this transformation is driven by the entanglement between conduction electrons and local f moments, producing heavy quasiparticles, reconstructed Fermi surfaces, and hybridization gaps. The same competition between Kondo screening and Ruderman-Kittel-Kasuya-Yosida exchange also underlies antiferromagnetism, quantum criticality, non-Fermi-liquid behavior, and unconventional superconductivity [1–3], while the emergence of the heavy-electron fluid follows a universal crossover phenomenology in many Kondo-lattice materials [4]. A central unresolved issue is therefore not only where Kondo coherence appears in equilibrium, but whether the resulting hybridized state is a rigid low-energy band structure or a fragile many-body configuration that can be dynamically reorganized.

This distinction is especially important in weakly hybridized Kondo lattices. In such systems, the hybridization gap is not merely an equilibrium energy scale; it reflects a delicate redistribution of f -electron spectral weight, magnetic correlations, and quasiparticle entropy, consistent with the broader view that heavy-electron behavior is governed by the progressive emergence and effectiveness of Kondo hybridization [5]. Static probes, including ARPES, scanning tunneling spectroscopy, optical spectroscopy, NMR/Knight-shift measurements, and quantum oscillations, have revealed that f -electron itinerancy in heavy-fermion systems is orbital selective, momentum dependent, and probe dependent [6–11]; in several Ce- and U-based compounds, it can even partially reverse at the lowest temperatures, with $4f/5f$ spectral weight showing delocalization or back transfer rather than a monotonic buildup of itinerant weight [12–17]. These observa-

tions challenge the view of Kondo coherence as a one-way crossover into a rigid heavy band. However, equilibrium spectroscopy cannot determine whether the low-temperature hybridized electronic structure is dynamically rigid or susceptible to nonequilibrium reconstruction. A decisive test requires a perturbation that acts on the electronic system before lattice thermalization and tracks how the low-energy quasiparticle spectrum recovers.

CePt₂In₇ provides a stringent platform for this test. It is a layered member of the Ce_{*m*}M_{*n*}In_{3*m*+2*n*} family and orders antiferromagnetically at $T_N = 5.2$ K, and becomes superconducting under pressure when magnetism is suppressed [18–26]. Compared with the more strongly hybridized Ce-115 compounds, CePt₂In₇ exhibits weak c - f hybridization [12, 27] and multiple low-energy scales. NMR suggests a coherence scale near 20 K [23], whereas Knight-shift analysis points to a higher crossover scale near 40 K and indicates partial $4f$ relocalization below ~ 14 K [17]. ARPES further reveals an unconventional evolution of Ce $4f$ spectral weight [12]. CePt₂In₇ therefore offers a rare opportunity to ask whether weak Kondo hybridization behaves as a fixed bottleneck or as a reconstructable electronic state tied to partial $4f$ relocalization and magnetic correlations.

Ultrafast spectroscopy offers a direct route to this issue. In a gapped or pseudogapped quasiparticle spectrum, recombination is constrained by a Rothwarf-Taylor bottleneck: photoexcited quasiparticles and high-frequency bosons exchange energy until the low-energy electronic depletion recovers [28–34]. The temperature dependence of this channel identifies the relevant recombination scale, while the pump-fluence dependence tests the rigidity of the underlying hybridized state. A fixed hybridization gap should produce sublinear growth, saturation, or gap filling [32–34]. By contrast, a fragile hybridized state may display a qualitative reversal of the fluence

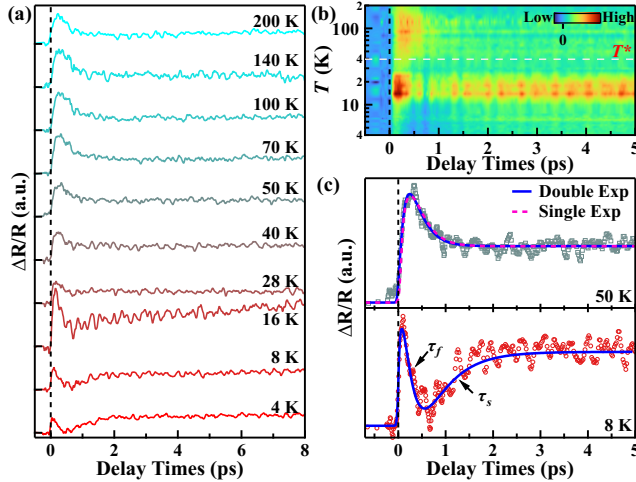


FIG. 1. Emergence of a slow hybridization-related relaxation channel in CePt_2In_7 . (a) Temperature-dependent transient reflectivity $\Delta R/R$ measured at a pump fluence of approximately $15 \mu\text{J}/\text{cm}^2$. Curves are vertically offset for clarity. (b) Pseudocolor map of $\Delta R/R$ as a function of temperature and delay time. The dashed line marks the crossover scale $T^* \sim 40 \text{ K}$, around which the delayed relaxation component gradually becomes resolvable. (c) Representative fits using Eq. (1). At 50 K, the slow component is weak and single- and double-exponential fits are nearly indistinguishable. At 8 K, the delayed dip-like response requires the two-component fit. Arrows indicate the fast and slow relaxation time scales, τ_f and τ_s , respectively.

response when photoexcitation redistributes low-energy spectral weight.

Here we uncover such a fluence-reversal fingerprint in CePt_2In_7 . Low-fluence dynamics reveal a slow hybridization-related relaxation channel below $T^* \sim 40 \text{ K}$ and a Rothwarf-Taylor bottleneck scale $2\Delta \approx 7.4 \text{ meV}$. Coherent optical phonons provide an internal lattice reference: their strong equilibrium thermal softening but negligible fluence-induced softening rule out large quasi-equilibrium lattice heating as the dominant origin of the nonlinear response. The decisive observation is the evolution of the phonon-free electronic amplitude A_{elec} . With cooling from the hybridization-crossover regime, A_{elec} first remains approximately linear in fluence, then develops a representative Rothwarf-Taylor-like sublinear response in the intermediate-temperature regime, and finally turns upward at the lowest temperatures under strong excitation. This reversal cannot be accounted for by a rigid fixed-gap bottleneck alone. Instead, it provides an ultrafast optical signature of photoinduced redistribution of a fragile Kondo-hybridized electronic response.

High-quality single crystals of CePt_2In_7 were grown by the In-flux method and freshly cleaved along the (001) surface before optical measurements. Femtosecond pump-probe reflectivity was performed under a vacuum of approximately 10^{-6} mbar using 800-nm pulses with a duration of about 35 fs from a 1-MHz Yb-based oscillator [35–37]. The pump and probe spot diameters were approximately 65 and 40 μm , respectively, with orthogonal polarizations. The transient reflectivity $\Delta R(t)/R$ was measured as a function of delay time, tempera-

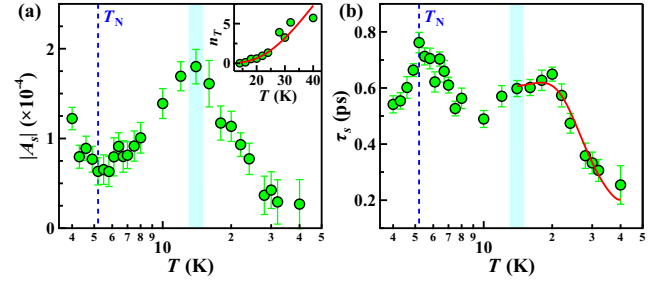


FIG. 2. Rothwarf-Taylor bottleneck analysis of the slow relaxation channel. (a) Temperature dependence of the slow-component amplitude $|A_s|$. The inset shows the thermally excited quasiparticle density n_T extracted from $|A_s|$. (b) Temperature dependence of the slow relaxation time τ_s . Red solid curves are Rothwarf-Taylor fits, yielding a low-energy bottleneck scale $2\Delta \approx 7.4 \text{ meV}$. The shaded region indicates the low-temperature reconstruction scale near $\sim 14 \text{ K}$.

ture, and pump fluence. Low-fluence temperature-dependent measurements were performed at approximately $15 \mu\text{J}/\text{cm}^2$, whereas fluence-dependent measurements extended up to $331 \mu\text{J}/\text{cm}^2$.

Figure 1(a) shows the low-fluence transient reflectivity $\Delta R(t)/R$ from 4 to 200 K. The response contains a prompt electronic component followed by a slower relaxation that becomes increasingly visible upon cooling. The temperature-delay map in Fig. 1(b) shows that this delayed channel develops continuously below a crossover scale near $T^* \sim 40 \text{ K}$. We fit the early-time dynamics using

$$\frac{\Delta R(t)}{R} = (1 - e^{-t/\tau_r})[A_f e^{-t/\tau_f} + A_s e^{-t/\tau_s} + C], \quad (1)$$

convoluted with the instrumental response. τ_r is the rise time, A_f and τ_f describe the fast component, A_s and τ_s describe the delayed channel, and C accounts for the long-lived background. At 50 K, single- and double-exponential fits are nearly indistinguishable, whereas at 8 K the delayed dip-like response requires the two-component form [Fig. 1(c)]. The full temperature-dependent data are shown in Supplemental Material Sec. S1 [38]. The fast component remains shorter than approximately 0.3 ps and is naturally assigned to the initial redistribution of photoexcited carriers through electron-boson scattering, as discussed in Supplemental Material Sec. S2 [38]. We therefore focus on the slow component as the optical signature of low-energy quasiparticle recombination in the weakly hybridized Kondo state.

The slow channel carries the thermodynamic fingerprint of Kondo hybridization. Figure 2 shows that both $|A_s|$ and τ_s become resolvable below $\sim 40 \text{ K}$ and develop a pronounced nonmonotonic structure: $|A_s|$ grows upon cooling, reaches a maximum near $\sim 14 \text{ K}$, is suppressed on approaching T_N , and then increases again at the lowest temperatures. Such behavior is not the response of a monotonically forming rigid heavy band. Instead, it indicates that the low-energy quasiparticle spectrum is reshaped by the competition between weak c - f hybridization, partial $4f$ relocation, and antiferromagnetic correlations.

To quantify the recombination scale, we analyze the slow component using a Rothwarf-Taylor bottleneck framework [34, 39, 40]. The relaxation rate and thermally excited quasiparticle density are written as

$$\tau^{-1}(T) = \Gamma[\delta(\varepsilon n_T + 1)^{-1} + 2n_T], \quad (2)$$

$$n_T(T) = \frac{A(0)}{A(T)} - 1 \propto (T\Delta)^p e^{(-\Delta/T)}, \quad (3)$$

where n_T is the thermally excited quasiparticle density, Γ , δ , and ε are temperature-independent parameters, and p describes the density-of-states profile near the depletion edge. Taking $p = 0.5$, appropriate for a BCS-like density-of-states profile [34], yields $2\Delta \approx 7.4$ meV. This value should be interpreted as a low-energy recombination scale, not as the full direct optical hybridization gap [32, 33]. The distinction is essential: time-resolved reflectivity is sensitive to the near- E_F quasiparticle depletion that controls recombination, whereas infrared spectroscopy probes the direct optical hybridization gap. The crossover near $T^* \sim 40$ K agrees with the Knight-shift scale and lies above the NMR coherence scale [17, 23], confirming that Kondo coherence in CePt₂In₇ is probe dependent and dynamically fragile.

A central issue in any ultrafast experiment on heavy fermions is whether the observed response is electronic or merely thermal. Because the quasiparticle effective mass is large and the low-energy scales are small, even modest optical excitation can transiently elevate the electronic temperature. We therefore separate three stages of the nonequilibrium process. First, the pump pulse creates a nonthermal carrier distribution that rapidly redistributes energy within the electronic and strongly coupled bosonic subsystems. Second, recombination across the low-energy hybridization-related depletion proceeds through a bottleneck, captured by the slow channel. Third, the lattice approaches a quasi-equilibrium temperature on longer time scales. In the language of a two- or three-temperature model, the electronic system and a subset of strongly coupled bosons can be driven far from equilibrium before the full lattice bath is appreciably heated; in heavy-fermion systems, this separation is further amplified by the anomalous electron-phonon relaxation associated with the heavy quasiparticle density of states [41].

Coherent phonons provide an internal clock and thermometer for this separation. Figure 3(a) shows a representative high-fluence transient trace at 4 K. After subtracting the nonoscillatory electronic background, the residual oscillatory component contains two coherent modes at $f_1 \approx 2.91$ THz and $f_2 \approx 4.38$ THz. Raman spectroscopy at 300 K resolves modes near 95.5 and 144.7 cm^{-1} (see details in Supplemental Material Sec. S3 [38]), corresponding to approximately 2.86 and 4.34 THz [Fig. 3(b)], in good agreement with the time-domain modes. These oscillations are therefore coherent optical phonons rather than collective amplitude modes of an electronic order parameter.

The phonon frequencies are strongly temperature dependent: f_1 softens from approximately 2.91 to 2.84 THz and

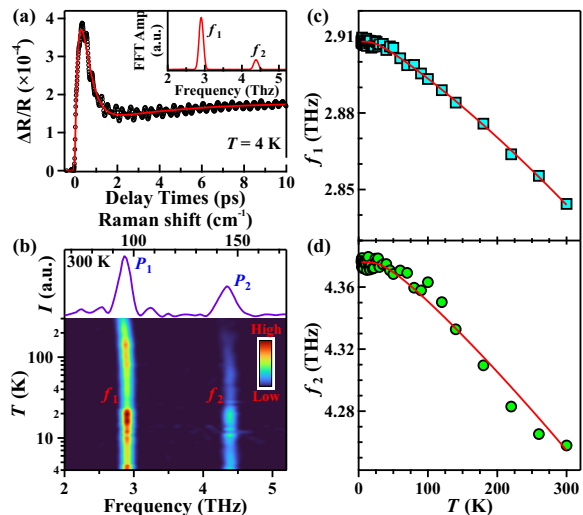


FIG. 3. Coherent optical phonons as an internal lattice reference. (a) Representative high-fluence transient reflectivity at 4 K. The red curve is the fitted nonoscillatory electronic background. The inset shows the Fourier spectrum of the residual oscillatory component, with coherent phonon modes at $f_1 \approx 2.91$ THz and $f_2 \approx 4.38$ THz. (b) Raman spectrum measured at 300 K and temperature-dependent FFT intensity map of the time-domain oscillations. The Raman modes near 95.5 and 144.7 cm^{-1} match the coherent phonons observed in pump-probe reflectivity. (c,d) Temperature dependence of f_1 and f_2 , respectively. Red curves are fits using an anharmonic phonon model.

f_2 from approximately 4.38 to 4.26 THz between 4 and 300 K [Figs. 3(c) and 3(d)]. Together with the damping rates in Supplemental Material Sec. S4 [38], this evolution is well described by a standard anharmonic phonon model [42, 43]. The same phonons, however, remain nearly fluence independent up to 331 $\mu\text{J}/\text{cm}^2$ [Fig. 4(b)]. This contrast rules out large quasi-equilibrium lattice heating as the dominant origin of the fluence-dependent electronic nonlinearity. It does not rule out an ultrafast hot-electron distribution immediately after excitation; rather, it shows that the electronic response cannot be collapsed onto a simple shift of the lattice temperature.

We now turn to the fluence dependence, which is the key nonequilibrium test. Figure 4(a) shows the transient reflectivity at 10 K. At low fluence, the signal retains the delayed dip-like recovery characteristic of the low-temperature hybridized state. With increasing fluence, the early dip is suppressed and a stronger delayed electronic component develops. The residual oscillatory signal also shows a delay-dependent period at high fluence, indicating that the photoexcited electronic potential transiently renormalizes the coherent lattice motion. This is precisely the regime in which electronic, bosonic, and lattice degrees of freedom are not yet described by a single temperature.

To isolate the electronic part of the response, we define A_{elec} as the peak amplitude of the fitted nonoscillatory background after removing the coherent phonon contribution. This definition minimizes contamination from the lattice oscillations and is tested by the background-subtracted quantity ($A_{\text{elec}} - C$) in

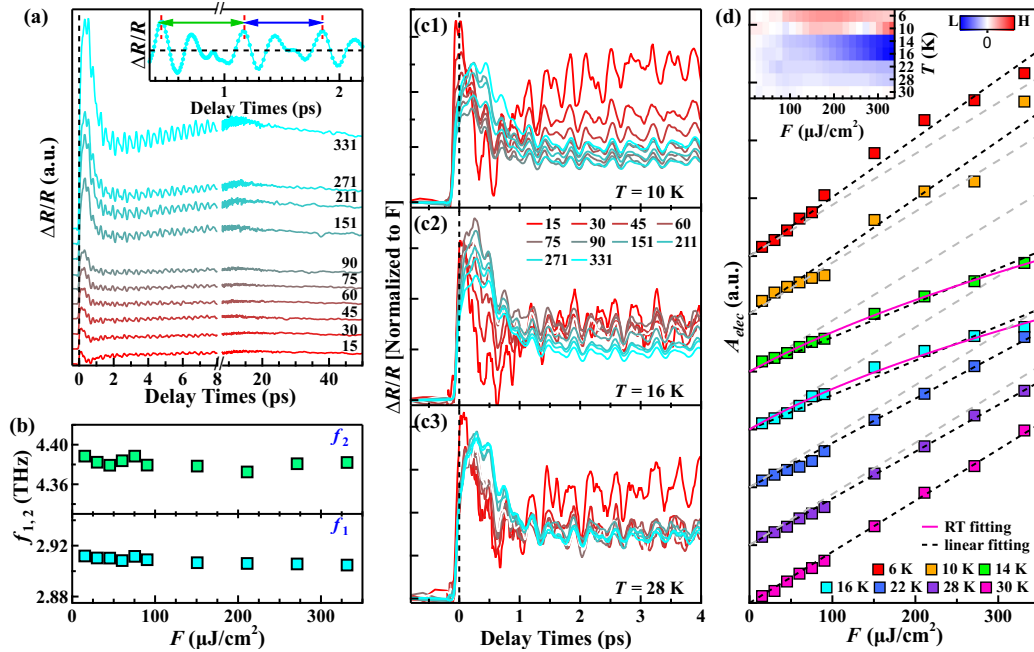


FIG. 4. Fluence-reversal fingerprint of fragile Kondo hybridization. (a) Fluence-dependent transient reflectivity $\Delta R/R$ at 10 K. Curves are vertically offset for clarity. The inset shows the residual oscillatory component at 331 $\mu\text{J}/\text{cm}^2$ after subtracting the nonoscillatory electronic background. (b) Fluence dependence of the coherent phonon frequencies f_1 and f_2 , showing negligible fluence-induced softening. (c1-c3) Fluence-normalized transient reflectivity $(\Delta R/R)/F$ at 10, 16, and 28 K. The lack of collapse demonstrates intrinsic nonlinear fluence dependence. (d) Fluence dependence of the fitted nonoscillatory electronic amplitude A_{elec} at 6, 10, 14, 16, 22, 28, and 30 K. Black dashed lines are linear fits; gray dashed lines are vertically shifted copies of the 30 K linear response; magenta solid curves are Rothwarf-Taylor fits to the 14 and 16 K data using Eq. (4). The inset shows the deviation map $\delta A(T, F) = A_{\text{elec}}(T, F) - A_{\text{elec}}^{\text{linear}}(30, F)$. The response evolves from a weak-linear regime at 30, 28, and 22 K, through a representative bottleneck-dominated sublinear regime at 14 and 16 K, to a low-temperature high-fluence enhancement regime at 10 and 6 K.

Supplemental Material Sec. S7 [38]. The fluence-normalized traces in Figs. 4(c1)-4(c3) do not collapse, demonstrating that the transient reflectivity is intrinsically nonlinear in fluence. The physical content of this nonlinearity is summarized by $A_{\text{elec}}(F)$ in Fig. 4(d).

The evolution of $A_{\text{elec}}(F)$ separates three nonequilibrium regimes. At 30 K, the response is nearly linear in fluence and provides the primary weak-hybridization reference. The 28 and 22 K data are also well described by linear functions, although they lie slightly below the 30 K reference. Thus, cooling within this regime does not yet produce a fully nonlinear bottleneck; instead, it gradually reduces the effective electronic susceptibility, consistent with the growth of a weak hybridization-related depletion of low-energy states.

Upon further cooling, the response enters a bottleneck-dominated regime. The 14 and 16 K data show representative sublinear fluence dependences and are well described by the Rothwarf-Taylor form [34]

$$A \propto \sqrt{1 + kF} - 1, \quad (4)$$

where k is a constant. We use these temperatures as representative examples of the intermediate-temperature bottleneck regime, not as the only temperatures that may follow an RT-like dependence. The agreement with Eq. (4) indicates that additional pump fluence produces fewer effective low-energy quasiparticles than expected for a linear metal-

lic response, because recombination is constrained by a depleted hybridization-related density of states. In nonequilibrium thermodynamic terms, the electronic subsystem does not simply absorb energy as a featureless metal; it stores and releases energy through a restricted quasiparticle-boson recombination channel.

The lowest temperatures show a qualitatively different response. At 10 and 6 K, the high-fluence data deviate upward from both the weak-linear reference and the RT-like sublinear trend. A fixed hybridization gap would naturally produce sublinear growth, saturation, or gap filling [32–34]. The observed enhancement therefore requires an additional electronic channel beyond a passive fixed-gap bottleneck. We attribute this channel to photoinduced redistribution of the fragile low-energy hybridized response. Below about 14 K, equilibrium Knight-shift measurements indicate partial relocalization of Ce $4f$ spectral weight [17]. In this regime, strong photoexcitation can perturb the balance among Kondo screening, partial $4f$ relocalization, and magnetic correlations. Rather than merely heating a pre-existing heavy band, the pump pulse transiently modifies the dielectric response associated with the low-energy Kondo-hybridized electronic structure.

This interpretation is supported by three consistency checks. First, the fluence reversal survives subtraction of the long-lived background C , as shown by $(A_{\text{elec}} - C)$ and $\delta(A_{\text{elec}} - C)$ in Supplemental Material Sec. S7 [38]. Second,

using either the 30 K or 28 K linear response as the weak-linear reference yields the same qualitative evolution: 22 and 28 K remain approximately linear, 14 and 16 K show sublinear suppression, and 10 and 6 K show positive high-fluence deviations. Third, the coherent phonon frequencies show negligible fluence-induced softening, excluding large quasi-equilibrium lattice heating as the dominant mechanism. The fluence reversal is therefore not a baseline artifact, not a coherent-phonon artifact, and not a simple lattice-heating effect.

The resulting physical picture is the following. Above the low-temperature reconstruction scale, photoexcitation probes a weakly hybridized but still approximately linear electronic response. Near the strongest slow-channel amplitude, quasi-particle recombination becomes bottlenecked by a low-energy hybridization-related depletion. At still lower temperatures, where partial $4f$ delocalization and magnetic correlations become increasingly relevant, strong excitation opens an additional nonequilibrium pathway: the hybridized response is no longer merely filled or saturated, but transiently redistributed. Time-resolved reflectivity does not directly measure the momentum-resolved $4f$ spectral function. Nevertheless, the robust fluence reversal of the phonon-free electronic amplitude provides an optical fingerprint of a reconstructable Kondo electronic state.

In summary, femtosecond pump-probe reflectivity reveals that weak Kondo hybridization in CePt_2In_7 is not a rigid low-temperature gap. Low-fluence quasiparticle dynamics identify a hybridization crossover near $T^* \sim 40$ K and a Rothwarf-Taylor recombination scale $2\Delta \approx 7.4$ meV. Coherent optical phonons establish that the nonlinear fluence response cannot be reduced to large quasi-equilibrium lattice heating. Most importantly, the electronic amplitude evolves from a weak-linear regime, through representative RT-like bottleneck suppression around 14–16 K, to anomalous high-fluence enhancement at 10 and 6 K. This reversal distinguishes a passive fixed-gap bottleneck from a fragile Kondo-hybridized response that can be redistributed by ultrafast excitation. It establishes fluence-dependent pump-probe spectroscopy as a sensitive dynamical probe of whether heavy-fermion hybridization behaves as a rigid quasiparticle gap or as a reconstructable nonequilibrium many-body state.

This work was supported by the National Natural Science Foundation of China (Grants No. 12574168 and No. 12074436), the National Key Research and Development Program of China (Grant No. 2022YFA1604204), the Beijing National Laboratory for Condensed Matter Physics (Grant No. 2024BNLCPKF001), and the Science and Technology Innovation Program of Hunan Province (Grant No. 2022RC3068).

* Corresponding author: jqmeng@csu.edu.cn

[1] P. Gegenwart, Q. Si, and F. Steglich, Quantum Criticality in Heavy-Fermion Metals, *Nature Physics* **4**, 186 (2008).

- [2] S. Kirchner, S. Paschen, Q. Chen, S. Wirth, D. Feng, J. D. Thompson, and Q. Si, Colloquium: Heavy-electron quantum criticality and single-particle spectroscopy, *Rev. Mod. Phys.* **92**, 011002 (2020).
- [3] S. Doniach, The Kondo lattice and weak antiferromagnetism, *Physica B+C* **91**, 231 (1977).
- [4] Y. F. Yang, Z. Fisk, H. O. Lee, J. D. Thompson, and D. Pines, Scaling the Kondo lattice, *Nature* **454**, 611 (2008).
- [5] Y. F. Yang and D. Pines, Emergent states in heavy-electron materials, *Proc. Natl. Acad. Sci.* **109**, E3060 (2012).
- [6] P. Aynajian, E. H. da Silva Neto, A. Gyenis, R. E. Baumbach, J. D. Thompson, Z. Fisk, E. D. Bauer, and A. Yazdani, Visualizing heavy fermions emerging in a quantum critical Kondo lattice, *Nature* **486**, 201 (2012).
- [7] Q. Y. Chen, D. F. Xu, X. H. Niu, J. Jiang, R. Peng, H. C. Xu, C. H. P. Wen, Z. F. Ding, K. Huang, L. Shu, Y. J. Zhang, H. Lee, V. N. Strocov, M. Shi, F. Bisti, T. Schmitt, Y. B. Huang, P. Dudin, X. C. Lai, S. Kirchner, H. Q. Yuan, and D. L. Feng, Direct observation of how the heavy-fermion state develops in CeCoIn_5 , *Phys. Rev. B* **96**, 045107 (2017).
- [8] Q. Y. Chen, D. F. Xu, X. H. Niu, R. Peng, H. C. Xu, C. H. P. Wen, X. Liu, L. Shu, S. Y. Tan, X. C. Lai, Y. J. Zhang, H. Lee, V. N. Strocov, F. Bisti, P. Dudin, J. X. Zhu, H. Q. Yuan, S. Kirchner, and D. L. Feng, Band dependent interlayer f -electron hybridization in CeRhIn_5 , *Phys. Rev. Lett.* **120**, 066403 (2018).
- [9] Q. Y. Chen, X. B. Luo, D. H. Xie, M. L. Li, X. Y. Ji, R. Zhou, Y. B. Huang, W. Zhang, W. Feng, Y. Zhang, L. Huang, Q. Q. Hao, Q. Liu, X. G. Zhu, Y. Liu, P. Zhang, X. C. Lai, Q. Si, and S. Y. Tan, Orbital-selective Kondo entanglement and antiferromagnetic order in USb_2 , *Phys. Rev. Lett.* **123**, 106402 (2019).
- [10] Y. Z. Zhao, J. J. Song, Q. Y. Wu, H. Liu, C. Zhang, B. Chen, H. Y. Zhang, Z. H. Chen, Y. B. Huang, X. Q. Ye, Y. H. Yuan, Y. X. Duan, J. He, and J. Q. Meng, Experimental observation of the significant difference between surface and bulk Kondo processes in Kondo lattice YbCu_2Si_2 , *Sci. China Phys. Mech. Astron.* **67**, 247413 (2024).
- [11] Y. Wu, Y. J. Zhang, F. Du, B. Shen, H. Zheng, Y. Fang, M. Smidman, C. Cao, F. Steglich, H. Q. Yuan, J. D. Denlinger, and Y. Liu, Anisotropic c - f hybridization in the ferromagnetic quantum critical metal CeRh_6Ge_4 , *Phys. Rev. Lett.* **126**, 216406 (2021).
- [12] Y. Luo, C. Zhang, Q. Y. Wu, F. Y. Wu, J. J. Song, W. Xia, Y. F. Guo, J. A. Ruzs, P. M. Oppeneer, T. Durakiewicz, Y. Z. Zhao, H. Liu, S. Zhu, Y. H. Yuan, X. F. Tang, J. He, S. Y. Tan, Y. B. Huang, Z. Sun, Y. Liu, H. Y. Liu, Y. X. Duan, and J. Q. Meng, Three-dimensional and temperature-dependent electronic structure of the heavy-fermion compound CePt_2In_7 studied by angle-resolved photoemission spectroscopy, *Phys. Rev. B* **101**, 115129 (2020).
- [13] P. Li, H. Q. Ye, Y. Hu, Y. Fang, Z. G. Xiao, Z. Z. Wu, Z. Y. Shan, R. P. Singh, G. Balakrishnan, D. W. Shen, Y. F. Yang, C. Cao, N. C. Plumb, M. Smidman, M. Shi, J. Kroha, H. Q. Yuan, F. Steglich, and Y. Liu, Photoemission signature of the competition between magnetic order and Kondo effect in CeCoGe_3 , *Phys. Rev. B* **107**, L201104 (2023).
- [14] F. Y. Wu, Q. Y. Wu, C. Zhang, Y. Luo, X. Q. Liu, Y. F. Xu, D. H. Lu, H. Makoto, H. Liu, Y. Z. Zhao, J. J. Song, Y. H. Yuan, H. Y. Liu, J. He, Y. X. Duan, Y. F. Guo, and J. Q. Meng, Itinerant to relocalized transition of f electrons in the Kondo Insulator CeRu_4Sn_6 , *Front. Phys.* **18**, 53304 (2023).
- [15] N. Azari, M. R. Goeks, M. Yakovlev, M. Abedi, S. R. Dunsiger, S. M. Thomas, J. D. Thompson, P. F. S. Rosa, and J. E. Sonier, μ^+ Knight shift in UTe_2 : Evidence for delocalization in a Kondo lattice, *Phys. Rev. B* **108**, L081103 (2023).

- [16] J. J. Song, C. Zhang, Q. Y. Wu, Y. Z. Zhao, J. Ruzs, J. J. Joyce, K. S. Graham, P. S. Riseborough, C. G. Olson, H. Liu, B. Chen, Y. H. Yuan, Y. X. Duan, P. H. Tobash, E. D. Bauer, P. M. Oppeneer, T. Durakiewicz, and J. Q. Meng, Relocalization of uranium $5f$ electrons in the antiferromagnetic heavy-fermion superconductor UPd_2Al_3 : Insights from angle-resolved photoemission spectroscopy, *Phys. Rev. B* **109**, 205114 (2024).
- [17] N. apRoberts-Warren, A. P. Dioguardi, A. C. Shockley, C. H. Lin, J. Crocker, P. Klavins, D. Pines, Y. F. Yang, and N. J. Curro, Kondo liquid emergence and relocalization in the approach to antiferromagnetic ordering in CePt_2In_7 , *Phys. Rev. B* **83**, 060408(R) (2011).
- [18] N. apRoberts-Warren, A. P. Dioguardi, A. C. Shockley, C. H. Lin, J. Crocker, P. Klavins, and N. J. Curro, Commensurate antiferromagnetism in CePt_2In_7 , a nearly two-dimensional heavy fermion system, *Phys. Rev. B* **81**, 180403(R) (2010).
- [19] H. Shishido, T. Yoshihara, D. Nagamiya, S. Noguchi, H. Fujiwara, and T. Ishida, Single crystal growth of new heavy fermion compounds CePt_2In_7 and Ce_2PtIn_8 , *J. Phys.: Conf. Ser.* **592**, 012007 (2015).
- [20] P. H. Tobash, F. Ronning, J. D. Thompson, B. L. Scott, P. J. W. Moll, B. Batlogg, and E. D. Bauer, Single crystal study of the heavy-fermion antiferromagnet CePt_2In_7 , *J. Phys.: Condens. Matter* **24**, 015601 (2012).
- [21] T. Klimczuk, O. Walter, L. MÜchler, J. W. Krizan, F. Kinnart, and R. J. Cava, Crystal structure and electronic structure of CePt_2In_7 , *J. Phys.: Condens. Matter* **26**, 402201 (2014).
- [22] M. Månsson, K. Prša, Y. Sassa, P. H. Tobash, E. D. Bauer, C. Rusu, D. Andreica, O. Tjernberg, K. Sedlak, M. Grioni, T. Durakiewicz, and J. Sugiyama, Magnetic order in the 2D heavy-fermion system CePt_2In_7 studied by μ^+ SR, *J. Phys.: Conf. Ser.* **551**, 012028 (2014).
- [23] H. Sakai, Y. Tokunaga, S. Kambe, H. Lee, V. A. Sidorov, P. H. Tobash, F. Ronning, E. D. Bauer, and J. D. Thompson, NMR/NQR study of pressure-induced superconductor CePt_2In_7 , *J. Phys.: Conf. Ser.* **391**, 012057 (2012).
- [24] H. Sakai, Y. Tokunaga, S. Kambe, H. Lee, V. A. Sidorov, P. H. Tobash, F. Ronning, E. D. Bauer, and J. D. Thompson, Stabilization of commensurate antiferromagnetism in CePt_2In_7 by pressure up to 2.4 GPa: ^{115}In NMR and NQR under zero field, *Phys. Rev. B* **83**, 140408(R) (2011).
- [25] H. Sakai, Y. Tokunaga, S. Kambe, F. Ronning, E. D. Bauer, and J. D. Thompson, Coexistence of antiferromagnetism with superconductivity in CePt_2In_7 : Microscopic phase diagram determined by ^{115}In NMR and NQR, *Phys. Rev. Lett.* **112**, 206401 (2014).
- [26] E. D. Bauer, H. O. Lee, V. A. Sidorov, N. Kurita, K. Gofryk, J. X. Zhu, F. Ronning, R. Movshovich, J. D. Thompson, and T. Park, Pressure-induced superconducting state and effective mass enhancement near the antiferromagnetic quantum critical point of CePt_2In_7 , *Phys. Rev. B* **81**, 180507(R) (2010).
- [27] B. Shen, L. Yu, K. Liu, S. P. Lyu, X. W. Jia, E. D. Bauer, J. D. Thompson, Y. Zhang, C. L. Wang, C. Hu, Y. Ding, X. Sun, Y. Hu, J. Liu, Q. Gao, L. Zhao, G. D. Liu, Z. Y. Xu, C. T. Chen, Z. Y. Lu, and X. J. Zhou, Electronic structure of heavy fermion system CePt_2In_7 from angle-resolved photoemission spectroscopy, *Chin. Phys. B* **26**, 077401 (2017).
- [28] J. Demsar, R. D. Averitt, K. H. Ahn, M. J. Graf, S. A. Trugman, V. V. Kabanov, J. L. Sarrao, and A. J. Taylor, Quasiparticle relaxation dynamics in heavy fermion compounds, *Phys. Rev. Lett.* **91**, 027401 (2003).
- [29] Y. P. Liu, Y. J. Zhang, J. J. Dong, H. Lee, Z. X. Wei, W. L. Zhang, C. Y. Chen, H. Q. Yuan, Y. Yang, and J. Qi, Hybridization dynamics in CeCoIn_5 revealed by ultrafast optical spectroscopy, *Phys. Rev. Lett.* **124**, 057404 (2020).
- [30] Y. H. Pei, Y. J. Zhang, Z. X. Wei, Y. X. Chen, K. Hu, Y. Yang, H. Q. Yuan, and J. Qi, Unveiling the hybridization process in a quantum critical ferromagnet by ultrafast optical spectroscopy, *Phys. Rev. B* **103**, L180409 (2021).
- [31] B. L. Tan, C. Zhang, Q. Y. Wu, G. H. Dong, H. Liu, B. Chen, J. J. Song, X. Y. Tian, Y. Zhou, H. Y. Liu, Y. X. Duan, Y. G. Shi, and J. Q. Meng, Anisotropic hybridization dynamics in the quasi-one-dimensional Kondo lattice CeCo_2Ga_8 revealed by ultrafast optical spectroscopy, *Front. Phys.* **20**, 044208 (2025).
- [32] Y. Z. Zhao, Q. Y. Wu, C. Zhang, B. Chen, W. Xia, J. J. Song, Y. H. Yuan, H. Liu, F. Y. Wu, X. Q. Ye, H. Y. Zhang, H. Huang, H. Y. Liu, Y. X. Duan, Y. F. Guo, J. He, and J. Q. Meng, Coupling of optical phonons with Kondo effect and magnetic order in the antiferromagnetic Kondo-lattice compound CeAuSb_2 , *Phys. Rev. B* **108**, 075115 (2023).
- [33] R. Y. Chen, S. J. Zhang, E. D. Bauer, J. D. Thompson, and N. L. Wang, Optical spectroscopy and ultrafast pump-probe studies on the heavy-fermion compound CePt_2In_7 , *Phys. Rev. B* **94**, 035161 (2016).
- [34] J. Demsar, J. L. Sarrao, and A. J. Taylor, Dynamics of photoexcited quasiparticles in heavy electron compounds, *J. Phys.: Condens. Matter* **18**, R281 (2006).
- [35] X. Q. Ye, H. Liu, Q. Y. Wu, C. Zhang, X. F. Tang, B. Chen, C. C. Shu, H. Y. Liu, Y. X. Duan, P. M. Oppeneer, and J. Q. Meng, Ultrafast phonon hardening and nonthermal lattice potential reconstruction in the charge-density-wave material 1T-TiSe_2 , *Sci. China Phys. Mech. Astron.* **69**, 267412 (2026).
- [36] C. Zhang, Q. Y. Wu, W. S. Hong, H. Liu, S. X. Zhu, J. J. Song, Y. Z. Zhao, F. Y. Wu, Z. T. Liu, S. Y. Liu, Y. H. Yuan, H. Huang, J. He, S. L. Li, H. Y. Liu, Y. X. Duan, H. Q. Luo, and J. Q. Meng, Ultrafast optical spectroscopy evidence of pseudogap and electron-phonon coupling in an iron-based superconductor $\text{KCa}_2\text{Fe}_4\text{As}_4\text{F}_2$, *Sci. China Phys. Mech. Astron.* **65**, 237411 (2022).
- [37] Q. Y. Wu, C. Zhang, B. Z. Li, H. Liu, J. J. Song, B. Chen, H. Y. Liu, Y. X. Duan, J. He, J. Liu, G. H. Cao, and J. Q. Meng, Interplay of electron-phonon coupling, pseudogap, and superconductivity in $\text{CsCa}_2\text{Fe}_4\text{As}_4\text{F}_2$ studied using ultrafast optical spectroscopy, *Phys. Rev. B* **111**, L081110 (2025).
- [38] See Supplemental Material for additional data of CePt_2In_7 .
- [39] A. Rothwarf and B. N. Taylor, Measurement of Recombination Lifetimes in Superconductors, *Phys. Rev. Lett.* **19**, 27 (1967).
- [40] V. V. Kabanov, J. Demsar, B. Podobnik, and D. Mihailovic, Quasiparticle relaxation dynamics in superconductors with different gap structures: Theory and experiments on $\text{YBa}_2\text{Cu}_3\text{O}_{7-\delta}$, *Phys. Rev. B* **59**, 1497 (1999).
- [41] K. H. Ahn, M. J. Graf, S. A. Trugman, J. Demsar, R. D. Averitt, J. L. Sarrao, and A. J. Taylor, Ultrafast quasiparticle relaxation dynamics in normal metals and heavy-fermion materials, *Phys. Rev. B* **69**, 045114 (2004).
- [42] M. Balkanski, R. F. Wallis, and E. Haro, Anharmonic effects in light scattering due to optical phonons in silicon, *Phys. Rev. B* **28**, 1928 (1983).
- [43] J. Menéndez and M. Cardona, Temperature dependence of the first-order Raman scattering by phonons in Si, Ge, and α -Sn: Anharmonic effects, *Phys. Rev. B* **29**, 2051 (1984).